

## **SYBR green-activated sorting of *Arabidopsis* pollen nuclei based on different DNA/RNA content**

Vera K. Schoft<sup>1\*</sup>, Nina Chumak<sup>1†</sup>, János Bindics<sup>1</sup>, Lucyna Slusarz<sup>1</sup>, David Twell<sup>2</sup>, Claudia Köhler<sup>3</sup>, and Hisashi Tamaru<sup>1\*</sup>

<sup>1</sup>Gregor Mendel Institute, Austrian Academy of Sciences, Vienna, 1030, Austria

<sup>2</sup>Department of Biology, University of Leicester, Leicester, LE1 7RH, UK

<sup>3</sup>Department of Plant Biology, Swedish University of Agricultural Sciences and Linnean Center of Plant Biology, Uppsala, SE-75007, Sweden

\*To whom correspondence should be addressed. Email: vera.schoft@gmi.oeaw.ac.at, or hisashi.tamaru@gmi.oeaw.ac.at

†Present address: Institute of Plant Biology, University of Zürich, Zürich, 8008, Switzerland

### **Key message**

Purification of pollen nuclei

### **Abstract**

**Germ cell epigenetics is a critical topic in plants and animals. The male gametophyte (pollen) of flowering plants is an attractive model in which to study genetic and epigenetic reprogramming during sexual reproduction, being composed of only two sperm cells contained within, its companion, vegetative cell. Here we describe a simple and efficient method to purify SYBR green stained sperm and vegetative cell nuclei of *Arabidopsis thaliana* pollen using fluorescence activated cell sorting (FACS) to analyze chromatin and RNA profiles. The method obviates generating transgenic lines expressing cell type-specific fluorescence reporters and facilitates functional genomic analysis of various mutant lines and accessions. We evaluate the purity and**

**quality of the sorted pollen nuclei and analyze the technique's molecular basis. Our results show that both DNA and RNA contents contribute to SYBR green activated nucleus sorting and RNA content differences impact on the separation of sperm and vegetative cell nuclei. We demonstrate the power of the approach by sorting wild-type and polyploid mutant sperm and vegetative cell nuclei from mitotic and meiotic mutants, which is not feasible using cell type-specific transgenic reporters. Our approach should be applicable to pollen nuclei of crop plants and possibly to cell/nucleus types and cell cycle phases of different species containing substantially different amounts of DNA and/or RNA.**

**Key words** SYBR green, fluorescence activated cell sorting (FACS), pollen, sperm nuclei, male gametophyte, *Arabidopsis*.

## **Introduction**

Research focusing on epigenetic regulation of germ cells and their companion cells is currently attracting substantial interest in both plant and animal systems (Feng et al. 2010; Guzzardo et al. 2013). Increasing evidence suggests that genome-wide epigenetic reprogramming, which occurs in the germ cell lineages, plays crucial roles in plant and mammalian development, gene imprinting, transposon silencing and genome stability across generations. The flowering plant *Arabidopsis thaliana* has emerged as one of the primary model systems in these studies for exploration of the mechanisms involved. The innovative concept is that multiple layers of dynamic epigenetic reconfigurations, including DNA demethylation, *de novo* DNA methylation, and remodeling of histones and their modifications, occur in plant companion cells of both female and male gametes, which serve to regulate their development and to reinforce transposon silencing in gametes (Calarco et al. 2012; Gehring et al. 2009; Hsieh et al. 2009; Ibarra et al. 2012; Pillot et al. 2010; Schoft et al. 2011; Schoft et al. 2009; Slotkin et al. 2009).

The three-cell plant male gametophyte (pollen) comprises two sperm cells and a vegetative cell, the companion cell of the sperm, separated by a single asymmetric mitosis. This simple cell

system provides a simple attractive model to investigate epigenetic reprogramming during gametogenesis. In stamens after meiosis, each haploid unicellular microspore undergoes an asymmetric mitosis to form a large terminally differentiated vegetative cell and a smaller generative cell, which have spectacularly different chromatin and developmental fates. The generative cell, engulfed in the cytoplasm of the vegetative cell, undergoes a second mitosis to produce two sperm cells, resulting in a unique 'two cells within one cell' structure (Twell et al. 1998; Verelst et al. 2007). The primary role of the vegetative cell in plant reproduction is to germinate and form a pollen tube that delivers the sperm cells to the female gametophyte for double fertilization. One of the two sperm cells fertilizes the egg cell, whereas the other fertilizes the central cell. The products of this double fertilization are the embryo and the endosperm, an extra-embryonic nutritive tissue comparable to the mammalian placenta. Despite its biological significance, the information on the epi/genomic and transcriptomic landscape of the plant male gametophyte genomes is limited. *Arabidopsis* provides excellent genetic and genomic resources to elucidate the function and mechanism of genetic and epigenetic reprogramming during pollen development. To achieve this goal, it is essential to purify large quantities of sperm and vegetative cell nuclei of pollen from plant lines in various genetic backgrounds.

SYBR green I is an asymmetrical cyanine dye (Zipper et al. 2004) that binds to nucleic acids and is used as a dye to quantify double stranded DNA (Simpson et al. 2000) and to label DNA within cells for fluorescence microscopy (Patel et al. 2007) and flow cytometry (Marie et al. 1997). Notably, SYBR green I also stains RNA with a lower affinity than DNA (Zipper et al. 2004). We established a simple and efficient method to disrupt pollen grains and fractionate sperm and vegetative cell nuclei using fluorescence activated cell sorting (FACS) based on differences in the intensity of their SYBR green I staining, and used it to show differences in DNA methylation patterns in *Arabidopsis* sperm and vegetative cells (Schoft et al. 2009). This method enables instant sorting of pure populations of the two nuclei types from various plant lines (e.g., T-DNA insertion mutants and different *Arabidopsis* accessions) without the need to generate transgenic lines expressing sperm- and vegetative cell-specific fluorescence reporters. This method therefore avoids any further disruption of the genome by transgene insertion and facilitates functional genetics and genomics. However, why SYBR green I staining could discriminate between the sperm and vegetative cell nuclei remains unclear.

Here, we give a detailed account of the protocol and report our advancement and qualitative

analysis of the SYBR green-activated pollen nuclei sorting. We evaluate the purity and quality of the FACS sorted populations and analyze the molecular basis underlying the technique. We describe protocols for isolation of DNA and RNA from sorted sperm and vegetative cell nuclei. Fluorescence and electron microscopic images of the sorted sperm fraction revealed nuclei that lack the plasma membrane, indicating that they are sperm nuclei, not sperm cells. Our results show that both DNA and RNA contents contribute to the SYBR green activated nuclei sorting, therefore, the separation of sperm and vegetative cell nuclei is, at least in part, based on differences in their RNA contents. We demonstrate the power of the approach by sorting wild-type and polyploid mutant sperm and vegetative cell nuclei from mitotic and meiotic mutants which is likely not possible using cell type specific transgenic fluorescence reporters.

## Materials and Methods

### Plant lines and growth conditions

We carried out electron microscopy and transcript analysis using wild-type *Arabidopsis thaliana* accession Columbia (Col-0). For assessing the purity of the sorted fractions a double homozygous line (Col-0) carrying *pCenH3::CenH3::GFP* and *pLAT52::H2B::RFP* (Schoft et al. 2009) was used. *DUO1/duo1-1* heterozygous plants were used for sorting pollen nuclei and *DUO1/duo1-1* heterozygous plants in a *qrt1/qrt1* background were used for pollen microscopy (Durberry et al. 2005). For assessing the integrity of sperm plasma membranes a line expressing *AtGEX2::eGFP* (Engel et al. 2005) was used. Diploid pollen was isolated from the *jas-3* mutant (Erilova et al. 2009). Plants were grown at 16-h light/8-h dark cycle at 22°C.

### Pollen isolation

We collected pure mature pollen samples from five week-old flowering plants as previously described (Honys 2003; Johnson-Brousseau 2004; Schoft et al. 2009) with modifications. Inflorescences from approximately 2000 plants were collected in a beaker, covered with 9% sucrose solution, and shaken vigorously for 1 min to release mature pollen grains into the solution. To remove larger debris, the pollen suspension was filtered through a 100 µm nylon mesh (Biologix, 15-1100). Pollen grains were precipitated in 250 ml centrifuge tubes using a Beckman Coulter Avanti J-26XP centrifuge with the JA-10 rotor (2800 rpm, 10 minutes at 4°C). The supernatant was added

back to the beaker containing the inflorescences, and the pollen harvesting procedure was repeated. To further purify pollen, the resulting two fractions of pollen pellet were resuspended in buffer A (1 M sorbitol, 7% ficol PM 400, 5 mM MgAc, 3 mM CaCl<sub>2</sub>, 5 mM EGTA, 50 mM Tris-HCl pH 7.5, 20 % glycerol and 2 % Triton X-100) and filtered through a 40 µm nylon mesh (Biologix, 15-1040) into a 15 ml Falcon tube. To prepare buffer A, all components except for glycerol and Triton X-100 were dissolved in water and the pH was adjusted to 7.5 with 1 M HCl. Finally, glycerol and Triton X-100 were added to the buffer. The solution can be used for 3-4 weeks when stored at 4°C. The two filtrates were pooled and concentrated by centrifugation (800 g, 10 minutes at 4°C). After a final wash step with 1ml of buffer A, the pollen was precipitated in a 1.5 ml centrifuge tube (7300 rpm, 5 minutes at 4°C in a table top centrifuge). A pollen pellet of 100 – 200 µl was obtained. The pellet can be used immediately or can be frozen in liquid nitrogen and stored at -80°C.

#### Isolation of pollen nuclei

To isolate nuclei of mature pollen grains, the rigid cell wall needs to be disrupted while at the same time keeping the nuclei intact. This was achieved by vortexing in the presence of glass beads. To this end, harvested pollen was resuspended in buffer A. Protease inhibitor cocktail (complete, EDTA-free protease inhibitor cocktail tablets (Roche, 11873580001) and PMSF (1mM final concentration) were added just before use. Pollen to buffer A ratios are critical for a successful sort: pollen pellets below a volume of 80 µl should be resuspended in a 1:3 ratio (pollen:buffer A), pollen volumes between 80 µl and 150 µl are best mixed in a 1:3.5 ratio and larger volumes in a 1:4 ratio. Deviations from this ratio resulted in either mostly unbroken pollen or damaged nuclei. 50 µl aliquots of pollen suspension were loaded onto 1.8 g of acid-washed glass beads (0.4-0.6 mm, Sartorius Stedim Biotech, BBI-8541701) in 2 ml centrifuge tubes, and subjected to bead beating using a Retsch MM301 ball mill for 1.5 minutes at a frequency of 15 Hertz. Subsequently, holes were punched with a needle (Ø 0.45 mm, Braun Petzold, 4657683) into the bottom of the tubes. The 2 ml tubes were placed on top of clean 1.5 ml centrifuge tubes and put into 15 ml centrifuge tubes. The pollen nuclei were collected into these 1.5 ml tubes by centrifugation (800 g, 10 minutes at 4°C). The glass beads containing tubes were discarded and the pollen nuclei suspensions were pooled in a clean 1.5 ml centrifuge tube using an air-displacement pipette. A DAPI-stained aliquot was inspected using a fluorescence microscope to assess the efficiency of pollen grain disruption and the quality of the free nuclei.

## Fractionation of sperm and vegetative cell nuclei by FACS

*Sample preparation for nucleus sorting:* The pollen nuclei suspension was diluted with 0.5 volumes of buffer B (15 mM Tris-HCl pH 7.5, 2 mM Na<sub>2</sub>-EDTA, 0.5 mM spermine-4 HCl, 80 mM KCl, 20 mM NaCl, 2% Triton X-100). PMSF (1 mM final concentration) and protease inhibitor cocktail solution (Roche, 11873580001) was added just before use. The sample was filtered through a 35 µm nylon mesh (BD Biosciences, 352235) into FACS tubes (250 µl per FACS tube). One sample was mixed with 5 µl of SYBR Green I (Invitrogen, S7567) and incubated on ice for 5 minutes. Additional samples were kept on ice and stained with SYBR green shortly before sorting.

For the Hoechst-Pyronin experiments, 5 µl of Hoechst33342 100 µg/ml (Sigma) was added to 50 µl of filtered pollen nuclei suspension containing 280 units of RNase inhibitor (RiboLock). After FACS, 5 µl of PyroninY 100µg/ml (Sigma) and 400 additional units of RNase inhibitor were added to 500 µl of purified pollen nuclei sample.

*FACS settings:* Fluorescence-activated cell sorting was carried out on a BD FACSAria I (Becton & Dickinson) with a 70 µm nozzle and 70 psi sheath pressure. The sample and the collected nuclei were cooled to 4°C during the whole procedure. A 488 nm Coherent Sapphire Solid State 13 mW Laser was used for excitation. SYBR green fluorescence was detected by a 530/30 nm bandpass filter, propidium iodide fluorescence was detected by a 610/620 nm bandpass filter. Hoechst 33342 was excited by UV laser and emission collected at 440/40 nm. Pyronin Y was excited at 488 nm and collected at 575/26nm. A sheath fluid standard BD FACS Flow solution was utilized. For analysis of parameters, the FACS Diva 6.1.2 software (Becton & Dickinson) was used.

## Pollen isolation (RNA protocol)

Flowers were collected from ~300, 4-6 weeks old Col-0 plants. Pollen was washed out with pollen isolation buffer (9 % m/v Sucrose, 25 mM Tris-HCl pH 7.5, 0.01 % v/v Triton X-100). The suspension was filtered through a 100 µm cell strainer and pollen was collected by centrifugation (1000 x g, 10 min, 4 °C). Then, pollen was resuspended in 10 ml Buffer A (50 mM Tris-HCl pH 7.5, 5 mM Mg(oAC)<sub>2</sub>, 3 mM CaCl<sub>2</sub>, 3 mM EGTA, 18.2 % m/v Sorbitol, 7 % m/v Ficoll PM400, 20 % v/v Glycerol, 2 % v/v Triton X-100) supplemented with 20 µl Protect™ RNA (Sigma) RNase inhibitor. The suspension was filtered through 40 µm cell strainer (Biologix Research Company, USA) and

pollen was collected by centrifugation (1000 x g, 10 min, 4 °C). Then, pollen was resuspended in 3ml Buffer A supplemented with 6 µl Protect™ RNA and distributed into 1.5 ml Eppendorf tubes to obtain ~30 µl pollen in each tube. Pollen was collected by centrifugation (1000 x g, 10 min, 4 °C) and supernatant was discarded. Wet pollen was flash-frozen in liquid N2 and stored at -80°C.

#### Vegetative and sperm nuclei isolation and FACS sorting (RNA protocol)

A frozen 30 µl aliquot of wet Arabidopsis pollen was resuspended in 1415 µl ice-cold Galbratih buffer (45 mM MgCl<sub>2</sub>, 30 mM Na Citrate, 20 mM MOPS, 1 % v/v Triton X-100, pH 7.0) supplemented with 15 µl 0.1 M PMSF (Sigma), 30 µl 50 x Complete EDTA-free Protease Inhibitor (Roche), 10 µl RiboLock RNase inhibitor (Thermo Scientific) and 60 µl glassbeads (0.4 – 0.6 mm). Pollen was disrupted by vortexing the suspension for 8 min at 4°C. Debris was removed by filtering the suspension through 10 µm cell strainer (CellTrics®, Partec). Nuclei were stained by 5 µl 10.000 x SYBR® Green I (Lonza) and subjected to FACS sorting. Sorted nuclei were collected into Trizol LS® (Life Technologies) reagent and subsequent RNA isolation was carried out according to the manufacturer's protocol.

#### Quality control of RNA obtained from pollen or sorted nuclei

Quality and quantity of RNA samples was determined using a Bioanalyzer 2100 instrument (Agilent Technologies) and the RNA 6000 Nano Kit RNA (Agilent Technologies) according to the manufacturer's instructions. Evaluation of the obtained electropherograms was done using the Plant total RNA assay.

#### RT-PCR

Detection of RNA transcripts were done using the OneStep RT-PCR kit (Qiagen) with minor modification of the manufacturer's instructions. The reactions were set up in 15 µl volume (8.6 µl H<sub>2</sub>O, 3 µl 5x buffer, 0.6 µl dNTP, 0.2 µl RiboLock RNase inhibitor (Thermo Scientific), 1 µl RNA template (7-10 ng), 1 µl primer mix (3.75 µM each)). Final concentration of each primer was 0.25 µM. We used the following thermal cycling program: 50°C 30min (reverse transcription - cDNA synthesis), 95°C 15min (activation of the hot-start PCR enzyme), 30x (94°C 30sec, 57.4°C 20sec, 72°C 75sec), 72°C 10min, 10°C hold.

PCR reactions were supplemented with 2  $\mu$ l 6x Orange Loading Dye (Thermo Scientific) and PCR products were separated by gel electrophoresis using 2% Agarose gel (Roth, Germany). Bands were visualized by Ethidium bromide (Roth, Germany) staining.

### Fluorescence microscopy

Microscopic images in Fig. 1 and 3 were taken with a Zeiss Axio Imager M1 fluorescence microscope equipped with differential interference contrast optics and a CCD camera (SPOT RT-KE, Diagnostic Instruments, USA). The image in Fig. 4 was taken with a Nikon Optiphot fluorescence microscope and CCD camera (KY-F55B, JVC, London) (Durberry 2005). Images in Fig. 2 and 5 were taken with a Zeiss Axioplan 2 fluorescence microscope and a CCD camera (CoolSNAP HQ2 Monochrome, Photometrics®). After each FACS, DAPI-stained sperm and vegetative cell nuclear populations were inspected for their purity based on differences in their size and morphology.

### Electron microscopy

Nuclei from Col-0 wild-type pollen were sorted as described above, except that to minimize further damage to sperm materials, sorted nuclei were collected into 1.5 ml tubes (500.000 nuclei per tube) containing 500  $\mu$ l of a nuclei protection buffer NPB (0.5 M sucrose, 20 mM Tris-HCl (pH8), 20 mM MgCl<sub>2</sub>, 0.3% Triton X-100, 1 x proteinase inhibitor cocktail and 1 mM PMSF). Nuclei were fixed in 1% paraformaldehyde in the same buffer for 6 minutes at room temperature and then centrifuged for 10 minutes (16100 g) in a tabletop centrifuge at 4°C. After centrifugation, the supernatant was carefully aspirated. The nuclei pellets were subjected to a second fixation step using 2.5% glutaraldehyde in a 0.1 M/l sodium phosphate buffer (pH 7.4) for 1 h at room temperature. The sample was rinsed with phosphate buffer, postfixed in 2% osmium tetroxide in the same buffer and washed with distilled water. The nuclei were dehydrated in a graded series of ethanol and embedded in Agar 100 resin. 70 nm sections then were cut and examined with a FEI Morgagni 268D (FEI, Eindhoven, The Netherlands) transmission electron microscope operated at 80 kV. Images were acquired using Morada CCD camera (Olympus-SIS).

## Results and discussion

### SYBR green-activated sorting of sperm and vegetative cell nuclei of pollen

To extract free intact sperm and vegetative cell nuclei, the rigid pollen cell wall needs to be disrupted. Beating pollen grains in buffer A (see Materials and Methods) in the presence of glass beads allowed efficient release of free pollen nuclei. Fig. 1a shows mature *Arabidopsis thaliana* pollen before disruption. After bead-beating, 80-90% of pollen grains are broken and pollen nuclei are released into the solution (Fig. 1b). The suspension containing unbroken pollen, debris of broken pollen and free nuclei was diluted with buffer B and then filtered through a 35  $\mu\text{m}$  mesh to remove large particles and aggregates that could clog the FACS tubing. Our method of sorting sperm and vegetative cell nuclei is primarily based on differences in their nucleic acid staining intensity. First, as a negative control, we checked a suspension of unstained free pollen nuclei in the flow cytometer and confirmed that no signal was detectable. SYBR green I or propidium iodide was then added to the sample and nuclei were sorted according to settings described in Materials and Methods. SYBR green I-stained nuclei emit green fluorescence on the fluorescein isothiocyanate (FITC) channel, whereas propidium iodide-stained nuclei emit red fluorescence on the PI channel. (Supplemental Figs. S1 a and b). Both dyes resulted in comparable FACS plots. In previous reports, we displayed all events in a graph showing SSC-A (side-scatter area) on the y-axis versus FITC-A (area) on the x-axis with a linear scale. Two fluorescent nuclear populations become visible, and we gated them separately (Fig. 1c). Using this procedure, we successfully sorted sperm and vegetative cell nuclei from various *A. thaliana* wild-type and mutants in different accessions to analyze DNA methylation at the gene and genomic level and transcription (Ibarra et al. 2012; Schoft et al. 2011; Schoft et al. 2009).

We further improved the SYBR green-activated pollen nucleus sorting to exclude unwanted events (e.g., two sperms adhered to each other) by using an auxiliary graph that displays FITC-W (FITC width) on the y-axis and FITC-A on the x-axis (Fig. 1d). Because aggregates possess a higher FITC-W value, we were able to distinguish them from single nuclei. The two populations shown in Fig. 1d were gated for sorting. We did not fix pollen nuclei with formaldehyde prior to FACS because we found that fixation resulted in the formation of large nuclear aggregates. Therefore, FACS was performed at 4°C to keep nuclei as intact as possible during sorting. Differences in nucleus size and intensity of fluorescence allowed us to distinguish sperm and vegetative cell nuclei under the microscope to assess the purity of each population.

To unambiguously evaluate the purity of the two nucleus populations, we took advantage of a double homozygous transgenic line expressing GFP-tagged CenH3 under the control of its native *CenH3* promoter and a RFP-tagged H2B driven by a vegetative cell-specific *LAT52* promoter in

mature pollen (Schoft et al. 2009). Mature pollen from the transgenic line display two sperm cell nuclei, containing five condensed CenH3-GFP centromeric foci and an RFP-positive vegetative cell nucleus (Fig. 1e). The vegetative cell nucleus undergoes loss of CenH3, coincident with extensive decondensation of centromeric heterochromatin at the binucleate pollen stage, thus showing no CenH3-GFP signals (Fig. 1e). Therefore, this transgenic line allows the identification of each pollen nucleus type under the fluorescence microscope after FACS (Schoft et al., 2009). We sorted half of the nuclear sample using propidium iodide staining to detect CenH3-GFP signals in sperm nuclei. Conversely, the other half sample was sorted by staining with SYBR green I to identify RFP-positive vegetative cell nuclei. It should be noted that both CenH3-GFP and H2B-RFP signals of sperm and vegetative nuclei were under the detection limit of the FACS device and did not interfere with SYBR green or propidium iodide-activated sorting. Using a fluorescence microscope we observed that the left and right populations in Fig. 1d contain nearly exclusively sperm and vegetative cell nuclei, respectively. The purity of both fractions was assessed to be >99%: the left fraction showed 630 sperms and 6 vegetative cell nuclei; the right fraction showed 1740 vegetative cell nuclei and 5 sperms (Fig. 1f). Besides high purity of each nucleus fraction, it contained little, if any, debris.

Our sorting protocol yields at least  $1 \times 10^6$  sperms and 350,000 vegetative cell nuclei, starting from 200 mg (~100  $\mu$ l) wet mature pollen material. The expected 2:1 ratio of sperm versus vegetative cell nuclei was not maintained during the overall sorting procedure, and this deteriorated slightly over time due to the increased susceptibility of vegetative cell nuclei to mechanical stress compared with sperm cell nuclei. This could be explained by the more fragile morphology of vegetative cell nuclei compared to sperm cell nuclei. Using this method, we have successfully sorted sperm and vegetative cell nuclei from various *A. thaliana* wild-type and mutants and accessions for DNA methylation studies (Supplementary Table S1; Supplementary Fig. S2).

In order to extend the application of the method to transcription and transcriptomic analyses of coding and non-coding RNAs, we established a protocol for obtaining high-quality RNA from sorted *A.thaliana* sperm and vegetative cell nuclei. To ensure RNA integrity we made the following adjustments to the procedure described above: Pollen isolation buffer (see Materials and Methods) was supplemented with Protect™ RNA (Sigma) RNase inhibitor. Nuclei were isolated in Galbraith buffer (see Materials and Methods) and sorted directly into Trizol. We performed chip-based capillary electrophoresis using a RNA 6000 Nano Bioanalyzer kit (Agilent, CA) to assess the quantity and quality of the RNA (Fig. 2a-c). Using our protocol, we obtained on average ~80 ng of

RNA /  $1 \times 10^6$  sperm nuclei and  $\sim 250$  ng of RNA /  $1 \times 10^6$  vegetative nuclei. Since the cytoplasm is lost during pollen nuclei purification, we assume that the majority of isolated sperm and vegetative cell RNA (Fig. 2 a and b) is nuclear/nascent RNA and chromatin-associated RNA, and that cytoplasmic RNA including mature ribosomal RNA which, represents major peaks in total pollen RNA (Fig. 2c), is underrepresented.

We conducted reverse transcription PCR (RT-PCR) analysis to compare transcripts derived specifically from sperm and vegetative cell nuclei. *DUO1* and *GEX2* are known to be preferentially expressed in the sperm (Rotman et al. 2005; Engel et al. 2005), whereas *UBQ10* is specifically expressed in the vegetative cell (Borges et al. 2008; Honys and Twell 2004). The isolated total RNA was used for one-step real time RT-PCR. We detected *DUO1* and *GEX2* exclusively in the sorted sperm nuclei, whereas *UBQ10* was detected exclusively in the sorted vegetative cell nuclei. (Fig. 2d). These data further confirm the purity of the two nuclei populations sorted by this method. *TUB4*, which is ubiquitously expressed in various tissues, was detected in both of the sorted nuclei samples and was used as a loading control (Fig. 2d). The optimized sorting protocol is suited to obtain pure total RNA from sorted *A. thaliana* sperm and vegetative pollen nuclei. The high yield of the RNA obtained from sorted pollen nuclei will allow high throughput total RNA and small RNA sequencing.

### **Purified sperm populations are sperm nuclei**

Pollen is a three-cellular structure with two sperm cells being engulfed in the cytoplasm of the vegetative cell. Disruption of pollen grains releases free nuclei from vegetative cells, though it remained unclear whether our bead beating and sorting procedures removed the plasma membrane of sperm cells. We therefore addressed the critical question whether the collected sperms were sperm cells, sperm nuclei, or a mixture of both. It is likely that the cell membrane integrity was lost during the preparation of nuclear extracts due to the presence of the detergent Triton X-100. In agreement with that, after the pollen disruption sperm nuclei could be stained with the plasma membrane impermeable dye propidium iodide (Supplemental Fig. 1 d). To assess the extent of cell membrane loss, we took advantage of an *A. thaliana* transgenic line expressing *Gex2* (At5g49150) fused to *eGFP* (Engel et al. 2005). *GEX2* is specifically expressed in the sperm cells in pollen and is bound to the plasma membrane (Fig. 3a). We detected GFP signals in 78% of total *GEX2* pollen grains analyzed. After disruption of pollen grains the sample was mixed with DAPI and the number of green fluorescent and non-fluorescent sperms was counted under the fluorescence microscope (Figs. 3b-c).

Nine GFP-positive (1.8%) and 500 GFP-negative (98.2%) sperm were observed, suggesting that most released sperm had lost their plasma membranes.

Adding further support to this notion, we prepared sorted sperm samples from wild-type *A. thaliana* plants for transmission electron microscopy (TEM). Analysis of the microscopic images in comparison with previously published TEM images of intact sperm cells within *A. thaliana* pollen (Owen and Makaroff 1995; Borg et al. 2014) revealed that all of the sorted sperms inspected (n = 413) completely lacked the plasma membrane (Fig. 3d). We conclude that the sperms purified by the procedure are not sperm cells, but sperm nuclei.

### **DNA content is a determinant for SYBR green-activated nucleus sorting**

We demonstrated above that staining pollen nuclei with the DNA/RNA dye, SYBR green I or, alternatively, propidium iodide is sufficient to fractionate sperm and vegetative cell nuclei by FACS based on differences in their relative fluorescence intensity. However, because both types of nuclei have a haploid (1n) genome, it remains unclear what causes the staining differences between the sperm and vegetative cell nuclei. It is known that SYBR green I binds not only DNA, but also to RNA. Thus, it is possible that the differential fluorescence intensity reflects differences in their DNA and/or RNA content. Moreover, it is reasonable to speculate that unequal compaction states of chromatin between the two nuclei types facilitate or impede the dye binding to chromosomal DNA or RNA.

To test whether differences in DNA content contribute to nuclei sorting we used pollen from a *DUO1/duo1* heterozygous mutant plant (Fig. 4a). After the first pollen mitosis, the *duo1* mutant generative cell undergoes DNA replication but not the second mitosis, resulting in a diploid (2n) sperm-like cell (Rotman et al. 2005). The sperm-like cell is unable to fertilize and only heterozygous *DUO1/duo1* mutants can be propagated. Further, *duo1* does not alter features of the vegetative cell (Durberry et al. 2005). To test whether our method was able to separate *DUO1* and *duo1* sperm and *DUO1/duo1* vegetative cell nuclei, free nuclei prepared from *DUO1/duo1* pollen were subjected to the SYBR green-activated sorting as described above. We detected three populations in the FACS plot (Fig. 4b) and collected each fraction separately. Since *duo1* has a C to T point mutation at position 812 of the gene, we could confirm the identity of each FACS-sorted nuclear cloud. We extracted DNA from each nuclear fraction, amplified a *DUO1* fragment across the position 812 by PCR, and sequenced the PCR products directly. Genotyping of the sorted nuclei revealed that we had

successfully separated wild-type sperm (1n) and *duo1* sperm-like (2n) nuclear populations based on DNA content (Fig. 4c). Importantly, vegetative cell (1n) nuclei showed intermediate levels of SYBR green fluorescence between these two populations in closer proximity to wild-type sperm nuclei. The higher fluorescence intensity of the vegetative cell nuclear clouds relative to the sperm nuclear clouds might reflect its higher DNA content and/or its extensively decondensed chromatin state (Schoft et al. 2009), which may enhance dye binding to chromosomal DNA. It is noteworthy that we did not collect the expected ratio of sorted nuclei of 2:2:1(SN:VN:*duo1*GCN). Apparently, not only vegetative cell nuclei but also *duo1* mutant sperm-like cell nuclei are more fragile than wild-type sperm nuclei during sorting. It is known that mutant cells without the DUO1 pathways fail to differentiate (Borg et al. 2014), which is caused by alterations in gene expression. As DUO1 target genes include genes coding for proteins that are localized to the plasma membrane and genes involved in chromatin structure (Borg et al. 2011), it is reasonable to assume that *duo1* mutant sperm-like cells could behave differently from wild-type sperm cells during purification steps. An experimental indication comes from the fact that, as for vegetative nuclei, the SN:VN:*duo1*GCN ratio deteriorates over time. Small scale sorts (<500000 SN) have, on average, a ratio of 5.0:1.9:1, whereas larger scale sorts (>500000 SN) have an averaged ratio of 11.3:6.2:1. Furthermore, gating was conservative to ensure clean populations, which may also contribute to slightly skewed ratios.

We further analyzed the performance of the SYBR green-activated nuclei sorting under the same conditions as described above using another *A. thaliana* mutant line homozygous for *jas3*, which results in more complex nuclear populations. While the *duo1* mutant forms diploid sperm-like cells but haploid vegetative cells, the meiotic *jason* (*jas*) mutant forms diploid pollen containing diploid sperm cells and diploid vegetative cells at about 60% frequency (De Storme and Geelen 2011; Eriova et al. 2009).

We detected four nuclear clouds, gated them, and sorted them separately (Fig. 5a). To examine the purity and identity of the four populations, 5 $\mu$ l of each sorted sample was stained with DAPI and >100 nuclei were evaluated under the fluorescence microscope. We were able to identify each nuclei population based on the size, shape, and DAPI/SYBR green staining intensity of nuclei (Fig. 5b). From left to right on the x-axis in ascending order of fluorescence intensity, 1n sperm, 1n vegetative, 2n sperm, and 2n vegetative cell nuclei were distributed (Fig. 5a). Results of 13 independent sorts are summarized in Supplementary Table S2. These data reinforce the notion that

DNA content is a strong basis for sorting SYBR green-stained nuclei, allowing the separation of wild-type and polyploid-mutant sperm and vegetative cell nuclei.

### **RNA content is a second determinant for SYBR green-activated pollen nuclei sorting**

The vegetative and sperm cells both have an active transcriptome of similar complexity, but the vegetative cell being significantly larger is dominant in terms of capacity for RNA production (Hony & Twell 2004; Borges et al 2008). SYBR green I binds not only DNA, but also RNA (Zipper et al. 2004). To investigate whether the differential SYBR green fluorescence staining between the sperm and vegetative cell nuclei is due to differences in their RNA content, we pretreated free pollen nuclei with RNase and then recorded the clouds of sperm and vegetative cell nuclei by FACS. Figs. 6a and b show dot-plots of a FACS run of the samples untreated or treated with RNase. A representative RNA gel for assessing RNA digestion efficiency is shown in Supplementary Fig. S3. Both the RNase-treated sperm and vegetative cell nuclear populations displayed a decrease in the SYBR green fluorescence intensity compared to the standard untreated sample. Notably, the shift of the vegetative cell nuclei population towards weaker fluorescence intensity after RNase treatment was more prominent than that of the sperm nuclei population, resulting in the two populations being closer. This indicates that higher RNA content of the vegetative cell nucleus relative to the sperm nucleus is a determining factor for the SYBR green-activated sorting of the sperm and vegetative cell nuclei of pollen.

We next used the Hoechst33342-Pyronin Y technique (Crissman et al. 1985; Shapiro 1981) to selectively investigate the effect of RNA on sorting of the sperm and vegetative cell nuclei. Hoechst 33342 is an exclusive DNA dye, while Pyronin Y binds to both DNA and RNA. In the presence of the Hoechst, Pyronin Y reaction with DNA is blocked, and thus Pyronin Y stains RNA only. When cells/nuclei are stained first with Hoechst 33342 and then with Pyronin Y, it is possible to distinguish and quantify the fluorescence from DNA and RNA. This method has been applied to separate cycling G1 cells from quiescent cells, which are arrested in extended G1 or G0 phase and contain a relatively lower amount of RNA (Gothot et al. 1997; Shen et al. 2008). Of note, pollen debris contamination in free nuclei samples generated strong autofluorescence using green wavelength excitation and interfered with the detection of Pyronin-stained pollen nuclei. Therefore, we first sorted and purified a fraction containing both sperm and vegetative cell nuclei with Hoechst 33342 staining using UV wavelength excitation in the presence of RNase inhibitor (Fig. 6c). We tested whether Hoechst

binding to DNA was saturated by adding a second dose of the dye and observed no further increase in the fluorescence intensity of the nuclear clouds. We then added Pyronin Y to the sorted nuclei sample and FACS sorted them using green wavelength excitation to measure the Pyronin Y fluorescence. The sperm and vegetative cell nuclei populations were separated by the Pyronin RNA staining, albeit showing broader distributions of nuclei with more variable fluorescence intensity compared to the Hoechst DNA staining (Fig. 6d). These data are consistent with the notion that higher RNA content in the vegetative cell nucleus relative to the sperm nucleus is a factor that contributes to the SYBR green-activated sorting of these two types of pollen nuclei.

Our results emphasize the power of the SYBR green-activated cell sorting that allows purification of pollen sperm and vegetative cell nuclei using single wavelength excitation. Unlike the method reported recently, which uses transgenic reporters (Borges et al. 2012), our approach relies simply on staining nuclei with the nucleic acid dye SYBR green I and has potential to instantly sort and purify these two types of nuclei based on differences in their granularity, size, and DNA and/or RNA content. Not having to build transgenic lines expressing cell type specific fluorescence reporters avoids the risk of disturbing the genome and cellular processes by insertion mutations and transgene expression and facilitates genetic, genomic, and transcriptomic studies using various mutants and accessions. (Supplementary Table S1).

Sperm and vegetative cells are separated developmentally by only two mitoses, yet they are dramatically different in their appearance, function and fate. We developed our sorting protocol to be able to investigate how these impressive changes are achieved. To this end, sperm and vegetative cells have to be analysed separately to obtain a detailed picture of their genetic, epigenetic, and transcriptomic state. This information will shed light on pollen functions such as pollen tube growth, fertilization, epi/genetic reprogramming and imprinting, the influence of the male gametophyte on the fitness of the offspring by controlling transposition, and the role of non-coding RNAs. The possibility to separate mutant pollen nuclei with altered ploidy is another great resource to study key pathways in pollen development and cell specification, and is not possible with any other method currently available.

We anticipate that the SYBR green-based FACS will be applicable to pollen nuclei of crop plants and more broadly to cell/nuclei types and cell cycle phases of different species that contain substantially different amounts of DNA and/or RNA.

## AUTHOR CONTRIBUTIONS

VKS, NC, JB and HT designed research. VKS, NC, JB and LS performed research. DT provided the *DUO1/duo1-1* mutant. CK provided the *jas-3/jas-3* mutant. VKS, NC, JB, DT, CK and HT wrote the paper.

## ACKNOWLEDGEMENT

We thank Gabriele Stengl and Gerald Schmauss from the BioOptics Facility for setting up and optimizing FACS and Nicole Fellner and Günter Resch from the Campus Science Support Facility for electron microscopy. We thank Georg Krohne for advice and suggestions. We thank Sheila McCormick for an *AtGEX2:eGFP* transgenic line and Marjorie Matzke for *nrpe1* and *drd3-1* seeds. VKS thanks Marc Berlinger for his support. This work was supported by Austrian Science Fund (FWF) Grants P21389-B03 and P24918-B21 (to H.T.).

## CONFLICT OF INTEREST

The authors declare that they have no conflict of interest.

## REFERENCES

- Borg M, Brownfield L, Khatab H, Sidorova A, Lingaya M, Twell D (2011) The R2R3 MYB Transcription Factor DUO1 Activates a Male Germline-Specific Regulon Essential for Sperm Cell Differentiation in Arabidopsis. *Plant Cell* 23: 534–549
- Borg M, Rutley N, Kagale S, Hamamura Y, Gherghinoiu M, Kumar S, Sari U, Esparza-Franco MA, Sakamoto W, Rozwadowski K, Higashiyama T, Twell D (2014) An EAR-Dependent Regulatory Module Promotes Male Germ Cell Division and Sperm Fertility in Arabidopsis. *Plant Cell* 26: 2098–2113
- Borges F, Gardner R, Lopes T, Calarco JP, Boavida LC, Slotkin RK, Martienssen RA, Becker JD (2012) FACS-based purification of Arabidopsis microspores, sperm cells and vegetative nuclei. *Plant Methods* 8:44
- Borges F, Gomes G, Gardner R, Moreno N, McCormick S, Feijo JA, Becker JD (2008) Comparative transcriptomics of Arabidopsis sperm cells. *Plant Physiol* 148:1168-1181

- Calarco JP, Borges F, Donoghue MT, Van Ex F, Jullien PE, Lopes T, Gardner R, Berger F, Feijo JA, Becker JD, Martienssen RA (2012) Reprogramming of DNA methylation in pollen guides epigenetic inheritance via small RNA. *Cell* 151:194-205
- Crissman HA, Darzynkiewicz Z, Tobey RA, Steinkamp JA (1985) Correlated measurements of DNA, RNA, and protein in individual cells by flow cytometry. *Science* 228:1321-1324
- De Storme N, Geelen D (2011) The Arabidopsis mutant jason produces unreduced first division restitution male gametes through a parallel/fused spindle mechanism in meiosis II. *Plant Physiol* 155:1403-1415
- Durbary A, Vizir I, Twell D (2005) Male germ line development in Arabidopsis. duo pollen mutants reveal gametophytic regulators of generative cell cycle progression. *Plant Physiol* 137:297-307
- Engel ML, Holmes-Davis R, McCormick S (2005) Green sperm. Identification of male gamete promoters in Arabidopsis. *Plant Physiol* 138:2124-2133
- Erilova A, Brownfield L, Exner V, Rosa M, Twell D, Mittelsten Scheid O, Hennig L, Kohler C (2009) Imprinting of the polycomb group gene MEDEA serves as a ploidy sensor in Arabidopsis. *PLoS Genet* 5:e1000663
- Feng S, Jacobsen SE, Reik W (2010) Epigenetic reprogramming in plant and animal development. *Science* 330:622-627
- Gehring M, Bubb KL, Henikoff S (2009) Extensive demethylation of repetitive elements during seed development underlies gene imprinting. *Science* 324:1447-1451
- Gothot A, Pyatt R, McMahon J, Rice S, Srour EF (1997) Functional heterogeneity of human CD34(+) cells isolated in subcompartments of the G0 /G1 phase of the cell cycle. *Blood* 90:4384-4393
- Guzzardo PM, Muerdter F, Hannon GJ (2013) The piRNA pathway in flies: highlights and future directions. *Curr Opin Genet Dev* 23:44-52
- Honys D, Twell D (2003) Comparative analysis of the Arabidopsis pollen transcriptome. *Plant Physiol* 132:640-652
- Honys D, Twell D (2004) Transcriptome analysis of haploid male gametophyte development in Arabidopsis. *Genome Biol* 5:R85
- Hsieh TF, Ibarra CA, Silva P, Zemach A, Eshed-Williams L, Fischer RL, Zilberman D (2009) Genome-wide demethylation of Arabidopsis endosperm. *Science* 324:1451-1454
- Ibarra CA, Feng X, Schoft VK, Hsieh TF, Uzawa R, Rodrigues JA, Zemach A, Chumak N, Machlicova A, Nishimura T, Rojas D, Fischer RL, Tamaru H, Zilberman D (2012) Active DNA demethylation in plant companion cells reinforces transposon methylation in gametes. *Science* 337:1360-1364
- Johnson-Brousseau SA, McCormick S (2004) A compendium of methods useful for characterizing Arabidopsis pollen mutants and gametophytically-expressed genes. *Plant J* 39:761-775
- Marie D, Partensky F, Jacquet S, Vaultot D (1997) Enumeration and Cell Cycle Analysis of Natural Populations of Marine Picoplankton by Flow Cytometry Using the Nucleic Acid Stain SYBR Green I. *Appl Environ Microbiol* 63:186-193
- Owen HA, Makaroff CA (1995) Ultrastructure of microsporogenesis and microgametogenesis in Arabidopsis thaliana (L.) Heynh. ecotype Wassilewskija (Brassicaceae). *Protoplasma* 185:7-21

- Patel A, Noble RT, Steele JA, Schwalbach MS, Hewson I, Fuhrman JA (2007) Virus and prokaryote enumeration from planktonic aquatic environments by epifluorescence microscopy with SYBR Green I. *Nat Protoc* 2:269-276
- Pillot M, Baroux C, Vazquez MA, Autran D, Leblanc O, Vielle-Calzada JP, Grossniklaus U, Grimanelli D (2010) Embryo and endosperm inherit distinct chromatin and transcriptional states from the female gametes in *Arabidopsis*. *Plant Cell* 22:307-320
- Rotman N, Durbarry A, Wardle A, Yang WC, Chaboud A, Faure JE, Berger F, Twell D (2005) A novel class of MYB factors controls sperm-cell formation in plants. *Current Biology* 15:244-248
- Schoft VK, Chumak N, Choi Y, Hannon M, Garcia-Aguilar M, Machlicova A, Slusarz L, Mosiolek M, Park JS, Park GT, Fischer RL, Tamaru H (2011) Function of the DEMETER DNA glycosylase in the *Arabidopsis thaliana* male gametophyte. *Proc Natl Acad Sci U S A* 108:8042-8047
- Schoft VK, Chumak N, Mosiolek M, Slusarz L, Komnenovic V, Brownfield L, Twell D, Kakutani T, Tamaru H (2009) Induction of RNA-directed DNA methylation upon decondensation of constitutive heterochromatin. *EMBO Rep* 10:1015-1021
- Shapiro HM (1981) Flow cytometric estimation of DNA and RNA content in intact cells stained with Hoechst 33342 and pyronin Y. *Cytometry* 2:143-150 DOI 10.1002/cyto.990020302
- Shen H, Boyer M, Cheng T (2008) Flow cytometry-based cell cycle measurement of mouse hematopoietic stem and progenitor cells. *Methods Mol Biol* 430:77-86
- Simpson DA, Feeney S, Boyle C, Stitt AW (2000) Retinal VEGF mRNA measured by SYBR green I fluorescence: A versatile approach to quantitative PCR. *Mol Vis* 6:178-183
- Slotkin RK, Vaughn M, Borges F, Tanurdzic M, Becker JD, Feijo JA, Martienssen RA (2009) Epigenetic reprogramming and small RNA silencing of transposable elements in pollen. *Cell* 136:461-472
- Twell D, Park SK, Lalanne E (1998) Asymmetric division and cell-fate determination in developing pollen. *Trends Plant Sci* 3:305-310
- Verelst W, Twell D, de Folter S, Immink R, Saedler H, Munster T (2007) MADS-complexes regulate transcriptome dynamics during pollen maturation. *Genome Biol* 8:R249
- Zipper H, Brunner H, Bernhagen J, Vitzthum F (2004) Investigations on DNA intercalation and surface binding by SYBR Green I, its structure determination and methodological implications. *Nucleic Acids Res* 32:e103

## FIGURES LEGENDS

**Fig. 1** Assessment of the purity of sorted sperm and vegetative cell nuclei. **(a)** Microscopic images of *A. thaliana* wild-type (Col-0) pollen before preparation of free nuclei. BF: brightfield image, DAPI: DAPI stained pollen. 40x magnification. Size bar: 25  $\mu\text{m}$ . **(b)** Microscopic images of *A. thaliana* wild-type pollen after bead beating. Arrows point to released nuclei. 40x magnification. Size bar: 25  $\mu\text{m}$ . **(c, d)** Dot-plots of pollen nuclei during sorting, displayed as side scatter versus FITC-A of all events on linear scales **(c)** and as FITC-W versus FITC-A of events

gated in C (**d**). Gated populations displayed in **d** were collected. (**e**) Fluorescence image of a pollen grain from a transgenic *A. thaliana* line carrying *pCenH3::CenH3::GFP* and *pLAT52::H2B::RFP*. Red: H2B-RFP is expressed in the vegetative cell nucleus; Green: CenH3-GFP decorates centromeres in the sperm cell nuclei. 100x magnification. (**f**) Percentage of sperm (green) or vegetative (red) cell nuclei contained in population 1 and 2, respectively. Numbers above the bars indicate the number of nuclei counted. The purity of each fraction was determined to be around 99%.

**Fig. 2** Analysis of RNA isolated from FACS-purified *A. thaliana* pollen nuclei. (**a-c**) Quality check of RNA isolated from wild-type (Col-0) purified sperm nuclei (**a**) and vegetative cell nuclei (**b**) by FACS and total pollen (**c**) using the Agilent 2100 Bioanalyzer. Representative RNA electropherograms are shown. Vertical lines point to nucleotide (nt) sizes of ladder standard (200, 500, 1000, 2000 and 4000) indicated above the top panel. A 25nt marker was added to each sample and to the ladder to align individual runs. 18S and 25S rRNA peaks in total pollen RNA are indicated (**c**). Right panels show representative microscopic images of the corresponding sorted nuclei (**a, b**) and intact pollen (**c**) populations. Scale bars represent 5  $\mu\text{m}$ . (**d**) Analysis of *UBQ10*, *DUO1*, *GEX2* and *TUB4* transcripts in total RNA from sorted sperm nuclei (left panel) and vegetative cell nuclei (right panel) by the RT-PCR. We used *DUO1* and *GEX2* RNA as sperm nucleus-specific markers and *UBQ10* RNA as a vegetative nucleus-specific marker. *TUB4* RNA, expressed in both sperm and vegetative cells, was used as a control for loading equivalent amounts of cDNA on gels. PCR without the reverse transcriptase step (-RT) was performed to test for contaminating DNA.

**Fig. 3** Assessment of membrane integrity of sorted sperms. (**a**) A representative microscopic image of sperm cells within an intact *AtGEX2::eGFP* pollen. Sperm cells show green fluorescence in their plasma membrane. GFP: GFP channel, DAPI: DAPI channel; size bar: 10  $\mu\text{m}$ . 100x magnification. (**b**) A representative microscopic image of a GFP-negative sperm (marked by arrow) released from broken *AtGEX2::eGFP* pollen. 98.23 % of free sperms showed no green fluorescence. GFP: GFP channel, DAPI: DAPI channel. (**c**) Enlarged image of the area marked in **b**. (**d**) Transmission Electron Microscopy (TEM) analysis of sorted sperm population.

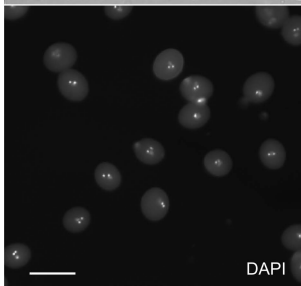
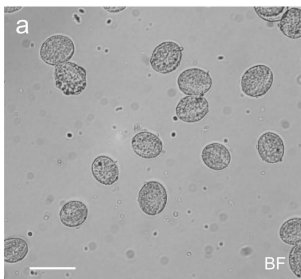
Three representative TEM images of sorted sperm nuclei lacking the plasma membrane are shown. Size bar: 500 nm. Magnification: 22000x.

**Fig. 4** SYBR green-activated sorting of *DUO1/duo1* pollen nuclei. **(a)** Segregation of wild-type (WT) and *duo1* pollen in a tetrad stained with DAPI from a *DUO1/duo1* heterozygous plant in a *qrt1/qrt1* background. **(b)** SYBR green-activated sorting of pollen nuclei from a *DUO1/duo1* heterozygous plant. Sperm nuclei (SN), vegetative cell nuclei (VN) and *duo1* sperm-like cell nuclei (GCN) were sorted based on differences in their SYBR green fluorescence intensity as displayed in a dot-plot. **(c)** Validation of the identity of each sorted nuclear population by sequencing.

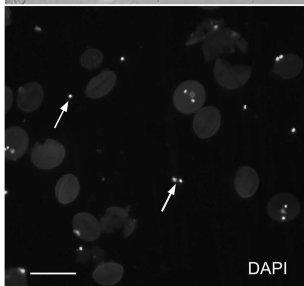
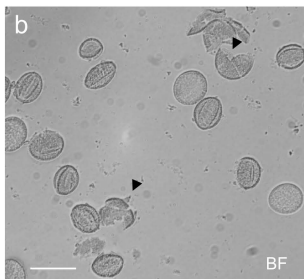
**Fig. 5** SYBR green-activated sorting of *jas-3* pollen nuclei. **(a)** SYBR green-activated cell-sorting of pollen nuclei from *jas-3/jas-3* homozygous mutant plants. 1n sperm (1n SN), 1n vegetative (1n VN), 2n sperm (2n SN), and 2n vegetative (2n VN) cell nuclei were sorted based on differences in their SYBR green fluorescence intensity as displayed in a dot-plot. **(b)** Microscopic pictures of sorted nuclei. Nuclei were counterstained with DAPI. Magnification 100x, Size bar 2 $\mu$ m.

**Fig. 6** RNA contributes to SYBR green-activated sorting of pollen nuclei. **(a and b)** Effects of RNase on SYBR green-activated nucleus sorting. Pollen nuclei (Col-0) were either untreated **(a)** or digested with RNase **(b)** prior to FACS. Displayed are side scatter versus fluorescence intensity on linear scales. The left population (sperm nuclei) and right population (vegetative nuclei) were gated. Gates were identical for both samples. **(c)** FACS of pollen nuclei with Hoechst 33342-DNA staining. Both sperm and vegetative cell nuclei were sorted and purified together using a single gate. **(d)** FACS of sperm and vegetative cell nuclei with Pyronin Y-RNA staining. Sperm nuclei (SN) and vegetative cell nuclei (VN) were sorted based on differences in their Pyronin Y staining as displayed in a dot-plot (upper panel) showing fluorescence intensity versus side-scatter and a histogram (lower panel) showing fluorescence intensity versus events-count of the gated sperm (blue) and vegetative cell (magenta) nuclear populations. Note that the horizontal x-axis is displayed in a logarithmic scale. RNA staining of nuclei with Pyronin Y

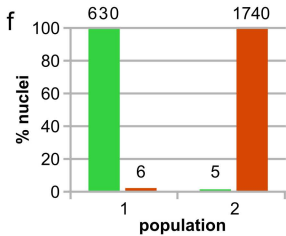
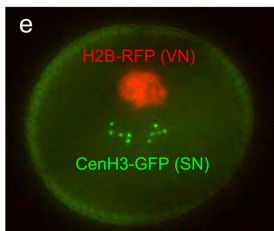
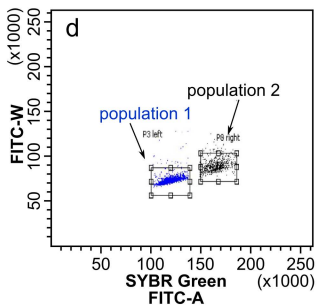
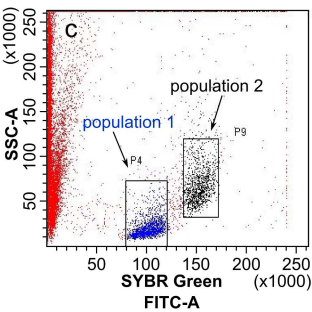
gives a broader range of events fluorescence intensity compared to DNA staining of nuclei with Hoechst 33342.

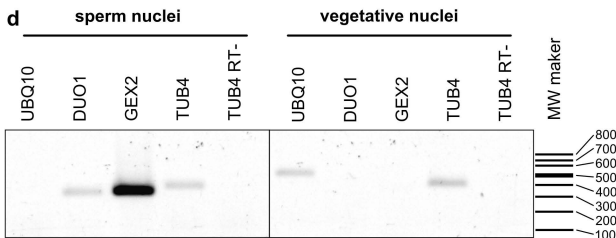
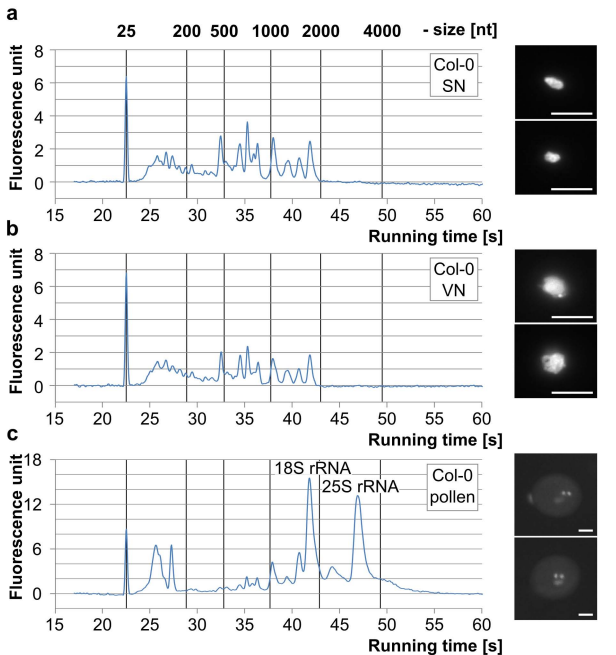


**Unbroken pollen**

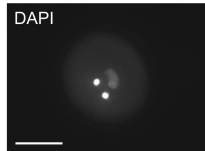
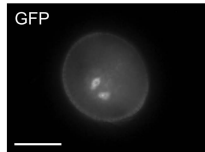


**Broken pollen**

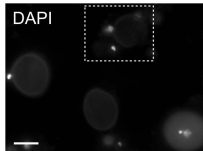
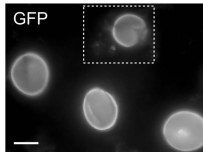




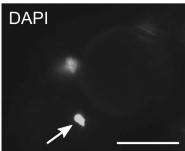
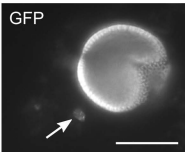
**a** unbroken pollen



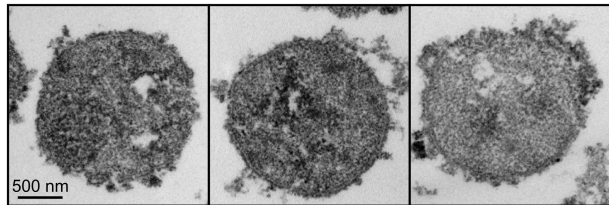
**b** broken pollen

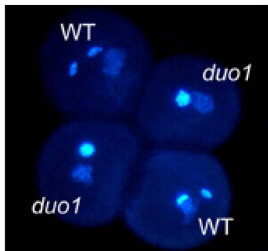
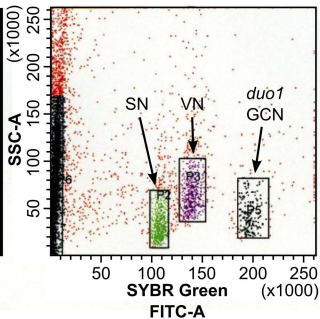
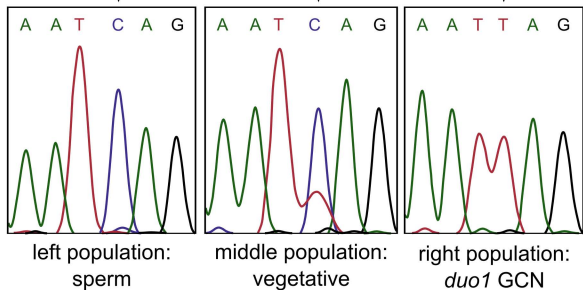


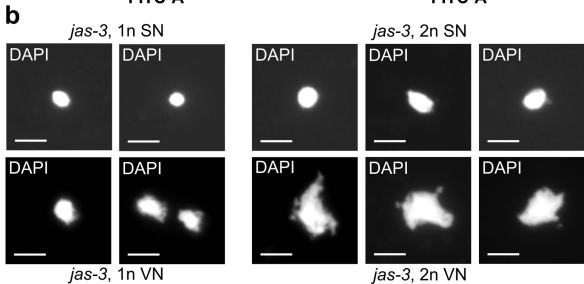
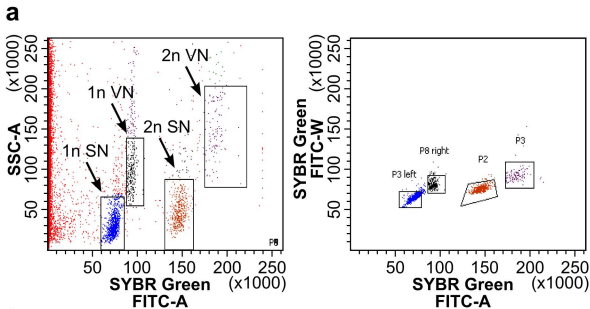
**c** broken pollen

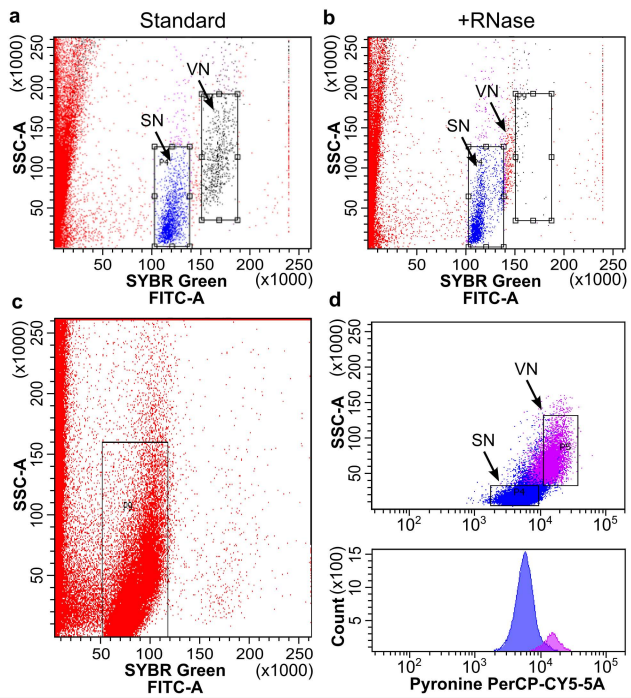


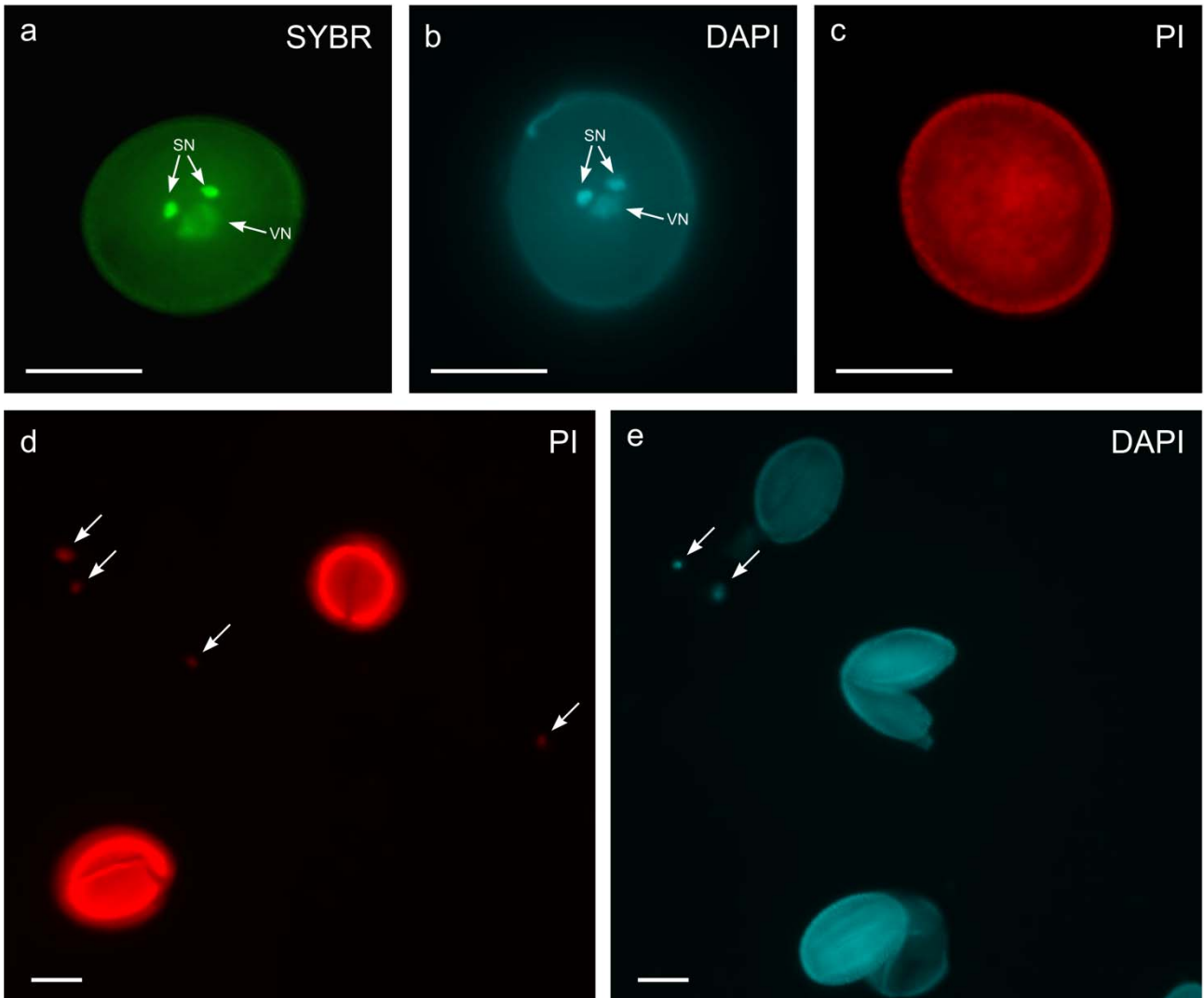
**d**



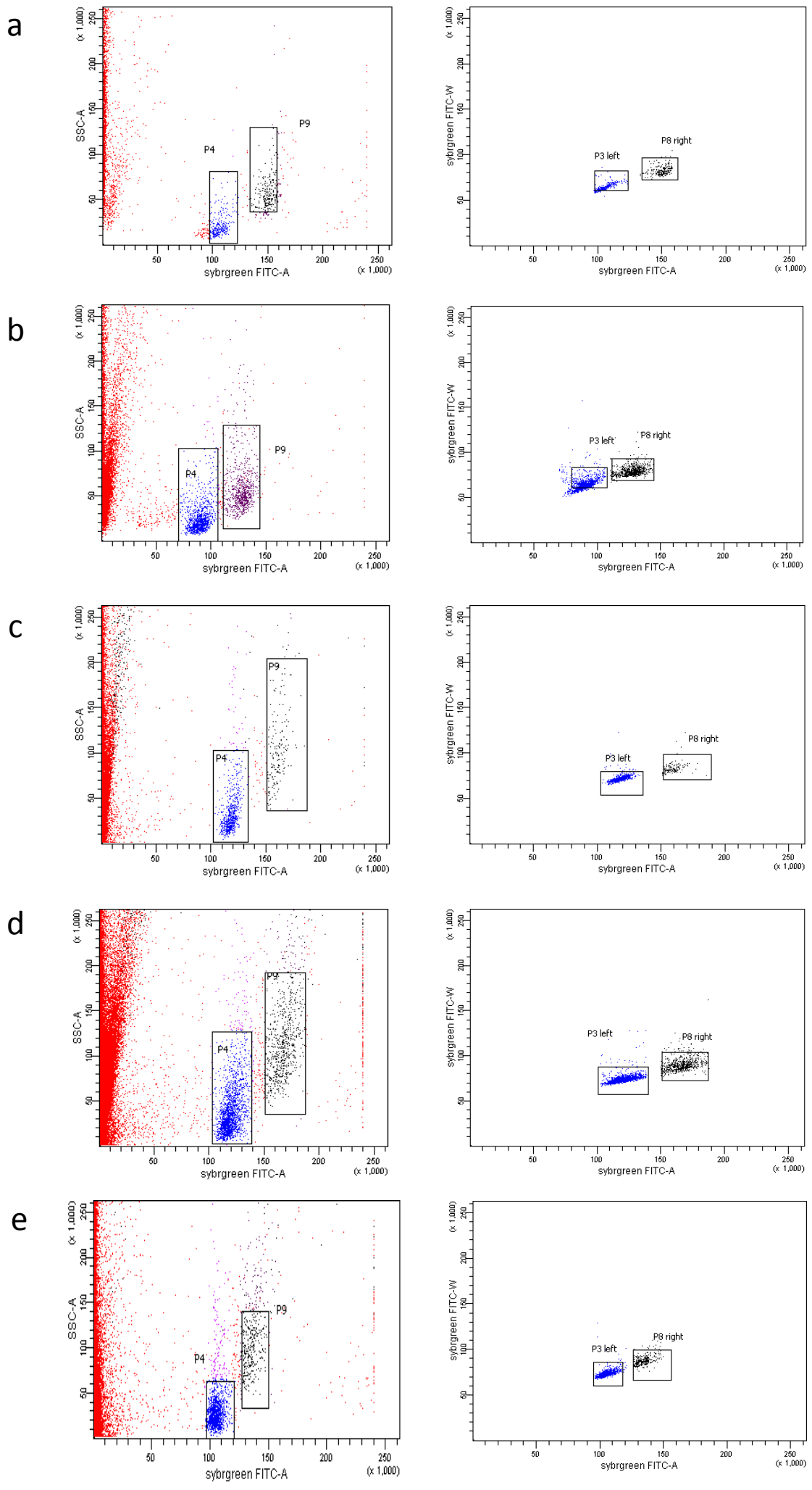
**a****b****c**







**Fig. S1** Fluorescence microscopic images of *Arabidopsis thaliana* wild-type (Col-0) pollen grains stained with (a) SYBR green I (SYBR), (b) DAPI, and (c) propidium iodide (PI), and captured at 63x magnification using the YFP filter (a), DAPI filter (b), and Texas red filter (c), respectively. SN, sperm cell nucleus; VN, vegetative cell nucleus. Size bars represent 10  $\mu\text{m}$ . (d) Fluorescence microscopic images of broken *A. thaliana* wild-type (Col-0) pollen grains and released sperm and vegetative cell nuclei stained with propidium iodide (PI) and captured at 20x magnification using the Texas red filter. Size bar is 10  $\mu\text{m}$ . Arrows point to released pollen nuclei. (e) Fluorescence microscopic images of broken *A. thaliana* wild-type (Col-0) pollen grains and released sperm and vegetative cell nuclei stained with DAPI and captured at 20x magnification using the DAPI filter. Size bar is 10  $\mu\text{m}$ . Arrows point to released pollen nuclei.



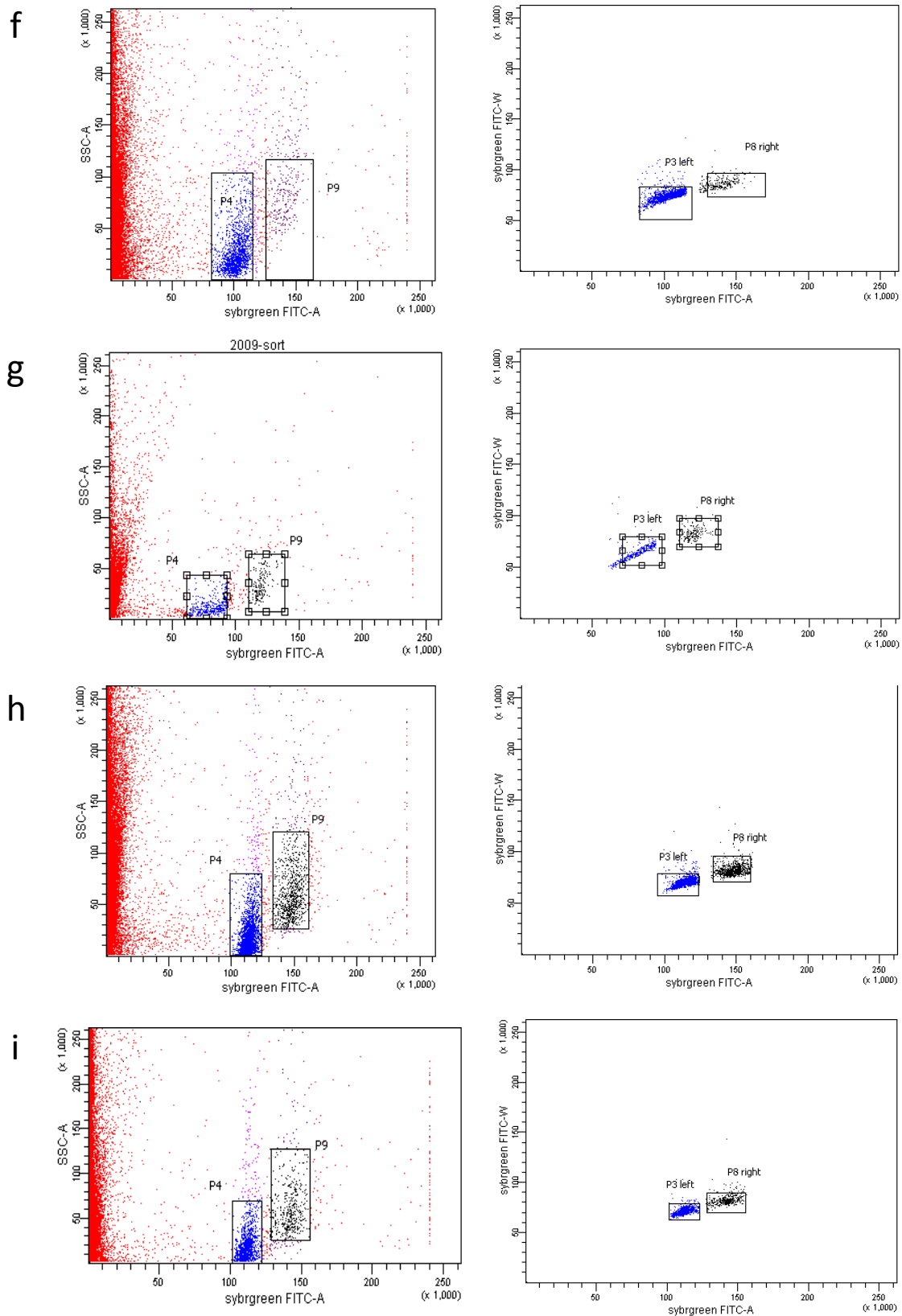


**Fig. S2** Representative FACS plots of *Arabidopsis* lines used for SYBR green activated cell sorting of pollen sperm and vegetative nuclei. (a) Col-0 wild-type, (b) *Ler* wild-type, (c) *WS* wild-type, (d) *nrpe1*, (e) *jmj27-1*, (f) *dme2* (*Ler*), (g) *ros1*, (h) *dml3*, (i) *ros1 dml2 dml3*.

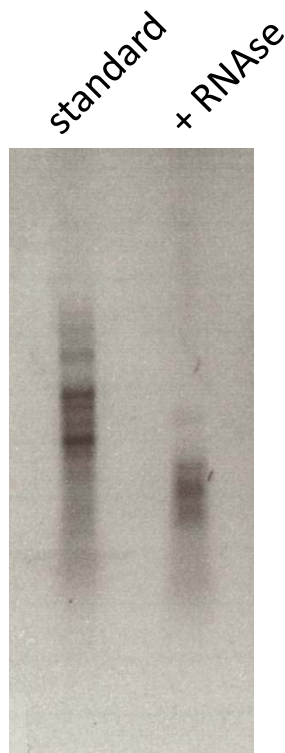


**Fig. S3** Efficiency of RNase digestion on FACS pollen samples.

RNA was isolated from pollen samples (treated with or without RNase) after recording of events to display FACS plots and run on a MOPS Northern gel. No RNase inhibitor was added to the standard sample, therefore, the RNA of the untreated sample is also partially degraded due to normal RNase contamination. The addition of RNase to the sample leads to a strong digestion of the RNA.

### Supplementary Materials and Methods

**Fig. S1 :**

Pollen staining procedures:

**SYBR Green I (LONZA)**

SYBR green I solution was diluted in Galbraith buffer 1:200. 5µl of this solution was mixed with 10µl pollen sample (suspended in Galbraith buffer) just before microscopy.

**DAPI:** A 0.6 µg/ml working concentration was used to stain pollen.

**Propidium iodide (Sigma):** A 2mg / ml stock dissolved in DMSO was prepared which was diluted 1:200 in Galbraith buffer. 1 µl of this solution was added to 14 µl pollen sample (suspended in Galbraith buffer) just before microscopy (0.6 µg/ml working concentration).

Images in Fig. S1 were taken with a Zeiss Axioplan 2 fluorescence microscope and a CCD camera (CoolSNAP HQ2 Monochrome, Photometrics). The images on Fig. S1 are false color representations of the monochrome images.

**Fig. S3 :**

The RNA was isolated from pollen samples, that were prepared for sorting and analyzed at the cell sorter, using PEQGOLD Trifast (PEQLAB, Germany) according to manual. RNA was separated on a MOPS Northern gel (adapted from Lehrach et al., 1977).

## Supplemented Table S1

List of *Arabidopsis* lines used in this and previous reports for SYBR green activated cell sorting of pollen sperm and vegetative nuclei (Ibarra CA et al. 2012, Schoft VK et al. 2011, Schoft VK et al. 2009).

LINE	ECOTYPE	GENE	FUNCTION
Col-0	Col-0	-	
Col-gl	Col-gl	-	
<i>Ler</i>	<i>Ler</i>	-	
WS	WS	-	
<i>cmt3</i>	Col-0	AT1G69770	Chromomethylase involved in methylating cytosine residues at non-CG sites.  Lindroth, A.M., Cao, X., Jackson, J.P., Zilberman, D., McCallum, C.M., Henikoff, S. and Jacobsen, S.E. (2001) Requirement of CHROMOMETHYLASE3 for maintenance of CpXpG methylation. <i>Science</i> , <b>292</b> (5524), 2077-80.
<i>ddm1</i>	Col-0	AT5G66750	SWI2/SNF2-like protein that acts as a chromatin-remodeling ATPase involved in cytosine methylation in CG and non-CG contexts.  Vongs, A., Kakutani, T., Martienssen, R.A. and Richards, E.J. (1993) <i>Arabidopsis thaliana</i> DNA methylation mutants. <i>Science</i> , <b>260</b> (5116), 1926-8.
<i>dme2</i>	<i>Ler</i>	AT5G04560	Encodes DNA glycosylase DEMETER. Protein is involved in active DNA demethylation.  Choi, Y., Gehring, M., Johnson, L., Hannon, M., Harada, J.J., Goldberg, R.B., Jacobsen, S.E. and Fischer, R.L. (2002) DEMETER, a DNA glycosylase domain protein, is required for endosperm gene imprinting and seed viability in arabidopsis. <i>Cell</i> , <b>110</b> (1), 33-42.
<i>dme2</i>	Col-gl	AT5G04560	Encodes DNA glycosylase DEMETER. Protein is involved in active DNA demethylation.  Choi, Y., Gehring, M., Johnson, L., Hannon, M., Harada, J.J., Goldberg, R.B., Jacobsen, S.E. and Fischer, R.L. (2002) DEMETER, a DNA glycosylase domain protein, is required for endosperm gene

			imprinting and seed viability in Arabidopsis. <i>Cell</i> , <b>110</b> (1), 33-42.
<i>dme6</i>	Col-0	AT5G04560	<p>Encodes DNA glycosylase DEMETER. Protein is involved in active DNA demethylation.</p> <p>Schoft, V.K., Chumak, N., Choi, Y., Hannon, M., Garcia-Aguilar, M., Machlicova, A., Slusarz, L., Mosiolek, M., Park, J.S., Park, G.T. <i>et al.</i> (2011) Function of the DEMETER DNA glycosylase in the Arabidopsis thaliana male gametophyte. <i>Proc Natl Acad Sci U S A</i>, <b>108</b>, 8042-8047.</p>
<i>dml2</i>	Col-0	AT3G10010	<p>Encodes DNA glycosylase DEMETER-like 2. Protein is involved in active DNA demethylation.</p> <p>Penterman, J., Zilberman, D., Huh, J.H., Ballinger, T., Henikoff, S. and Fischer, R.L. (2007) DNA demethylation in the Arabidopsis genome. <i>Proc Natl Acad Sci U S A</i>, <b>104</b>(16), 6752-7.</p>
<i>dml3</i>	Col-0	AT4G34060	<p>Encodes DNA glycosylase DEMETER-like 3. Protein is involved in active DNA demethylation.</p> <p>Penterman, J., Zilberman, D., Huh, J.H., Ballinger, T., Henikoff, S. and Fischer, R.L. (2007) DNA demethylation in the Arabidopsis genome. <i>Proc Natl Acad Sci U S A</i>, <b>104</b>(16), 6752-7.</p>
<i>drm1 drm2</i>	WS	AT5G15380 AT5G14620	<p>Methyltransferases involved in the <i>de novo</i> DNA methylation and maintenance of asymmetric methylation of DNA sequences.</p> <p>Cao, X. and Jacobsen, S.E. (2002) Role of the Arabidopsis DRM methyltransferases in <i>de novo</i> DNA methylation and gene silencing. <i>Curr Biol</i>, <b>12</b>, 1138-1144.</p>
<i>drm2</i>	Col-0	AT5G14620	<p>Methyltransferase involved in the <i>de novo</i> DNA methylation and maintenance of asymmetric methylation of DNA sequences.</p> <p>Cao, X. and Jacobsen, S.E. (2002) Role of the Arabidopsis DRM methyltransferases in <i>de novo</i> DNA methylation and gene silencing. <i>Curr Biol</i>, <b>12</b>, 1138-1144.</p>
<i>duo1</i>	No-0	AT3G60460	<p>R2R3 myb transcription factor that is required for male gamete formation, specifically for entry of the generative cell into mitosis.</p> <p>Rotman, N., Durbarry, A., Wardle, A., Yang, W.C., Chaboud, A., Faure, J.E., Berger, F. and Twell, D. (2005) A novel class of MYB factors controls sperm-cell formation in plants. <i>Current Biology</i>, <b>15</b>, 244-248.</p>

<i>jmj27</i>	Col-0	At4G00990	Jumonji (jmjC) domain-containing protein.
<i>nrpd1</i>	Col-0	AT1G63020	Encodes the largest subunit of the plant-specific RNA polymerase IV. Herr, A.J., Jensen, M.B., Dalmay, T. and Baulcombe, D.C. (2005) RNA polymerase IV directs silencing of endogenous DNA. <i>Science</i> , <b>308</b> , 118–120.
<i>nrpe1</i>	Col-0	AT2G40030	Encodes the largest subunit of the plant-specific RNA polymerase V. Kanno, T., Huettel, B., Mette, M.F., Aufsatz, W., Jaligot, E., Daxinger, L., Kreil, D.P., Matzke, M. and Matzke, A.J. (2005) Atypical RNA polymerase subunits required for RNA-directed DNA methylation. <i>Nat Genet</i> , <b>37</b> , 761–765.
<i>ros1</i>	Col-0	AT2G36490	Encodes DNA glycosylase ROS1. Protein is involved in active DNA demethylation. Gong, Z., Morales-Ruiz, T., Ariza, R.R., Roldán-Arjona, T., David, L. and Zhu, J.K.. (2002) ROS1, a Repressor of Transcriptional Gene Silencing in <i>Arabidopsis</i> , Encodes a DNA Glycosylase/Lyase. <i>Cell</i> , <b>111</b> (6), 803–814.
<i>ros1 dml2 dml3</i>	Col-0	AT2G36490 AT3G10010 AT4G34060	Triple mutant showing defects in DNA demethylation. Penterman, J., Zilberman, D., Huh, J.H., Ballinger, T., Henikoff, S. and Fischer, R.L. (2007) DNA demethylation in the <i>Arabidopsis</i> genome. <i>Proc Natl Acad Sci U S A</i> , <b>104</b> (16), 6752-7.
<i>Jas-3</i>			Encodes a protein of unknown function required for meiosis II. De Storme, N. and Geelen, D. (2011) The <i>Arabidopsis</i> mutant jason produces unreduced first division restitution male gametes through a parallel/fused spindle mechanism in meiosis II. <i>Plant Physiol</i> , <b>155</b> , 1403-1415.

## Supplemented Table S2

Validation of the purity of each sorted *jas-3* nuclear population by visual assessment.

5µl of each sorted sample was checked under the microscope. Nuclei were stained with DAPI (and SYBR green) and approximately 100 (or all available) nuclei were evaluated. Results of 13 sorts are summarized in this table. Nuclei were categorized to be of the expected type, of a different type or unidentifiable.

<b>population</b>	<b>expected nuclei</b>	<b>different type of nuclei</b>	<b>unidentifiable nuclei</b>
<b>1n SN</b>	1298	11	33
<b>1n VN</b>	901	56	24
<b>2n SN</b>	1099	52	32
<b>2n VN</b>	672	28	13

Ibarra CA, Feng X, Schoft VK, Hsieh TF, Uzawa R, Rodrigues JA, Zemach A, Chumak N, Machlicova A, Nishimura T, Rojas D, Fischer RL, Tamaru H, Zilberman D (2012) Active DNA demethylation in plant companion cells reinforces transposon methylation in gametes. *Science* 337:1360-1364

Schoft VK, Chumak N, Choi Y, Hannon M, Garcia-Aguilar M, Machlicova A, Slusarz L, Mosiolek M, Park JS, Park GT, Fischer RL, Tamaru H (2011) Function of the DEMETER DNA glycosylase in the *Arabidopsis thaliana* male gametophyte. *Proc Natl Acad Sci U S A* 108:8042-8047

Schoft VK, Chumak N, Mosiolek M, Slusarz L, Komnenovic V, Brownfield L, Twell D, Kakutani T, Tamaru H (2009) Induction of RNA-directed DNA methylation upon decondensation of constitutive heterochromatin. *EMBO Rep* 10:1015-1021